

PACS numbers: 52.50.Jm; 52.35.Dm
DOI: 10.1070/QE2003v033n09ABEH002506

Generation of a low-frequency wave by an optical discharge moving in a gas at a subsonic speed

V.N. Tishchenko

***Abstract*. A pulsating optical discharge moving in air at a subsonic speed ($\sim 250 - 300$ m s^{-1}) and creating in front of it a high-intensity low-frequency wave propagating in the same direction is considered. The range of dimensionless parameters in which this effect is manifested is determined.**

Keywords: *laser radiation, optical discharge, shock wave*.

In order to study the possibility of using laser radiation to control the flight of objects [1 – 3], a pulsating optical discharge (POD) was created in the supersonic gas flow [4] by laser radiation with a high pulse repetition rate ($f \sim$ 50 kHz), which reduced the aerodynamic resistance to about half [5]. A microwave laser discharge – the POD-induced trace of an ionised gas absorbing microwave radiation of higher power, was studied in Refs [6, 7]. This raises hopes of creating moving regions in a gas where new effects based on high energy density in laser plasma and a high frequency of its pulsation can be realised. The propagation of a POD corresponds to the displacement of the laser radiation focus at which a discharge operates. For large values of f, the POD acquires new properties that are not possessed by a continuous optical discharge (COD) or a solitary laser spark.

In contrast to a COD [8 – 10], a POD glows at gas flow velocities ranging from tens of metres per second to ~ 500 m s^{-1} (experiments at higher velocities were not conducted), absorbing $\sim 80\%$ of the laser radiation power [11]. The POD plasma decays slowly over a time $1/f$ and leaves a continuous trace of a high-temperature low-density gas. Acceleration of laser plasma in a POD and the generation of gas-dynamic perturbations whose spectrum can vary from infrasonic frequencies to hundreds of kilohertz appear to be quite interesting effects [12, 13]. A POD propagating at supersonic velocities can create a plasma jet in the opposite direction with a velocity as high as ~ 3 km s^{-1} [12]. A plasma jet (of length ~ 1 cm) was earlier observed during the expansion of a solitary laser spark [14, 15].

V.N. Tishchenko Institute of Laser Physics, Siberian Branch, Russian Academy of Sciences, prosp. Akad. Lavrent'eva 13/3, 630090 Novosibirsk, Russia; e-mail: tischenko@plasma.nsk.ru

Received 9 September 2002; revision received 25 November 2002; in final form 3 February 2003
Kvantovaya Elektronika **33** (9) 823 – 830 (2003)
Translated by Ram Wadhwa

The waves generated by a laser spark have been studied quite extensively (see, for example, Refs [16 – 20]). Generation of sound as a result of interaction of periodic laser pulses with water surface was studied in Refs [21 – 29]. Flux perturbations caused by an electric discharge at a pulse repetition rate of several hundred hertzs were studied in Refs [30, 31]. It was shown in Ref. [32] that interaction of shock waves (SWs) generated by a stationary POD can lead to the formation of a unified wave. This requires a high power and a high pulsation rate of a POD for which the wavelength of a SW is larger than the characteristic length C_0/f (where C_0 is the velocity of sound in the unperturbed gas). These conditions are close to the conditions prevailing in experiments [13, 32] in which a stationary POD operating in a narrow jet of argon produced periodic SW trains in air. The pressure spectrum contained ultrasonic and low-frequency components corresponding to the pulse repetition rate in the trains and to the repetition frequency of the trains. The laser power and the values of f were inadequate for creating a unified SW. However, the ratio of powers of low-frequency and ultrasonic components of pressure in the trains was much higher than in parametric radiators (the region of interaction of two ultrasonic beams in them emits waves with the difference frequency), considered to be among the most effective devices for generating low-frequency waves [33 – 37].

In this paper, we consider for the first time the formation of a low-frequency quasi-stationary wave (QW) formed in front of a POD propagating in air at a subsonic velocity $V_0 \sim 250 - 300$ m s^{-1}. For a point-size POD (spark length $\sim 1 - 2$ cm), the QW is formed as a result of interaction of periodic SWs generated by this discharge. In the direction of motion of the POD, shock waves successively catch up with one another and create a unified QW whose length increases with time on account of summation of a large number of SWs. In contrast to a compression wave, a QW is not a shock wave (the pressure in the QW is maximum at the trailing edge) and is not transformed into one as long as the pulsating optical discharge is operative. As a result of injection of energy into the supersonic flux, the shock waves may form a unified SW [1, 5, 12], but it will not be a low-frequency wave.

Our aim is to study the formation of a low-frequency QW and to find the range of parameters for which a POD can produce such a wave. Investigations were carried out by computer simulation since the creation of a QW requires a powerful radiation. The length of a QW may attain values for which the measurements of pressure in the wave as well as computations become complicated. Therefore, a simplified model was used and the initial stage of a QW (up to

~ 1.5 m, dozens of sparks) was studied. However, it was shown that the length of a QW increases linearly with time and becomes much larger than the characteristic sizes of parameters in the problem, viz., the spark length, dynamic range, and length of the SW produced by laser sparks. In this work, we solve the gasdynamic equations for the case of axial symmetry [38]. Data from Ref. [39] were used in the equation of state for air. Computation of each version took up to 100 h and more (using a computer with a processor clock frequency of 930 MHz). This model can be used for describing SWs since radiation losses of energy from a laser spark to air are small ($\sim 6\,\%$) [40], while the characteristic cooling time due to turbulent diffusivity is of the order of a few milliseconds [6]. Estimates show that these processes do not affect the QW significantly since the heating of the surrounding gas caused by them takes place behind the trailing edge of the QW.

A pulsating optical discharge in a gas can be produced by periodic laser radiation with a high pulse repetition rate ($\sim 20 - 100$ kHz) [13]. The shape of solitary sparks is nearly conical and depends on the angle of focusing of radiation as well as its power. To attain a high degree of concurrence of the obtained results and to extend them over a wide range of problems, we have assumed in our work that the sparks are spherical in shape. Such an assumption is valid in the problem on formation of a QW since the shape of a SW produced by an individual spark is nearly spherical at distances exceeding the spark length (extended 'bead-like' sparks are not considered). The duration of energy supply into atmospheric air (pressure $P_0 = 1$ atm, velocity of sound $C_0 = 340$ m s^{-1}) is taken equal to ~ 1 μs, and the spark radius R_0 is $0.3-1$ cm. The relative energy ε of sparks (ratio of the energy absorbed in a spark to the internal energy of the unperturbed gas in a volume equal to the volume of the spark) varied from 25 to 250. The spark energy Q_f and the energy density q_f in the spark are connected with ε through the relations $Q_f = \pi R_0^3 P_0 \varepsilon / 9.87(\gamma_0 - 1) = 1.06 P_0 R_0^3 \varepsilon$, $q_f/P_0 = 0.1013\varepsilon/(\gamma_0 - 1) = 0.253\varepsilon$. Here, the adiabatic index $\gamma_0 = 1.4$, R_0 is measured in centimetres, P_0 in atmospheres, Q_f in joules, and q_f in J cm^{-3}. The velocity of a moving POD is equal to the ratio of the distance between the spark centres to the laser pulse repetition period: $V_0 = Z_f/T_p$ ($T_p = 1/f$). The parameters V_0, T_p, ε and R_0 were varied during calculations.

Formation of quasi-stationary waves. Fig. 1 shows the theoretical SW fields for a subsonic propagation of a POD. At the instant $t = 0$, the centre of the first spark is located at the point $z = 0$, beyond which the sparks are created along the z axis of the motion of the POD (from right to left) at an interval $Z_f = V_0 T_p$. The sparks generate SWs which carry $\sim 40\,\%$ of the energy of laser plasma. The perturbed gas region is confined by a sphere which is the SW produced by the first spark and propagates with the velocity of sound C_0 in the unperturbed gas (for $t > 500$ μs). In the axisymmetric case, the preferred axis is the z axis along which the POD moves, and the centre of the sphere corresponds to the first spark. No QW is formed for small values of V_0, and the structure of the SW field is similar to the field produced by an acoustic source (Doppler effect). For $V_0 \geqslant 250$ m s^{-1} (depending on the energy of the sparks) and for Z_f below a certain value, SWs combine successively to form a QW along the direction of motion of a POD.

In the opposite direction, the SWs interact with the trailing edge of the QW and with the plasma trace left by the

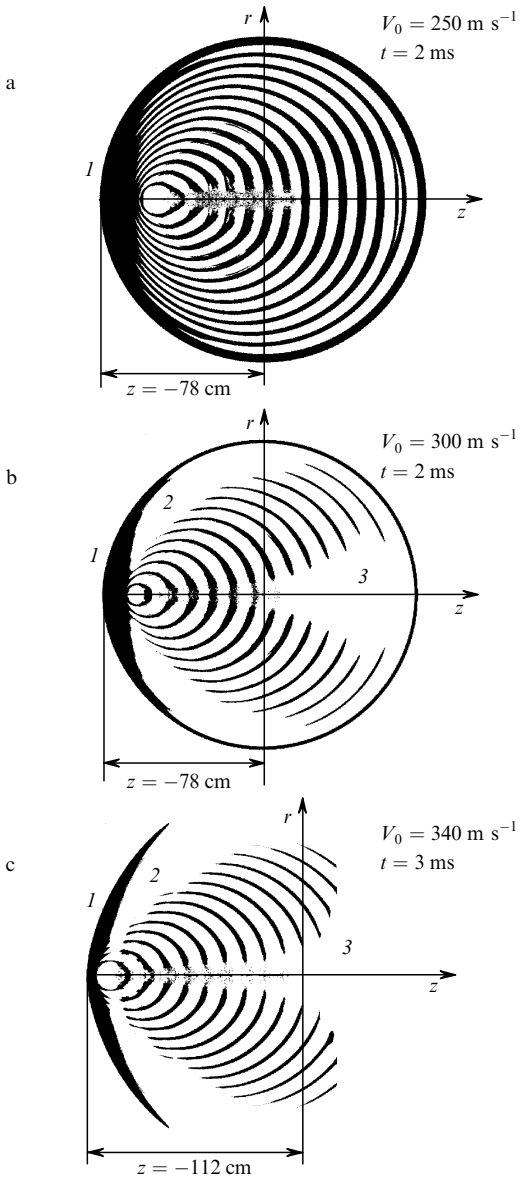

Figure 1. SW fields for different velocities of a POD at the instants $t \approx 2$ (a, b) and 3 ms (c) for a QW pressure much higher than the pressure in periodic SWs, $R_0 = 1$ cm, $\varepsilon = 25$, and $T_p = 0.15$ ms. The dark regions (*1*) correspond to the compression phases ($P > P_0$) of the shock waves and the quasi-stationary wave; (*2*) correspond to the low-pressure phase ($P < P_0$); and (*3*) to the 'shadow' region with a low pressure in the SW. The POD moves along the z axis from the point $z = 0$ (intersection of z and r axes) to the left with a velocity V_0.

POD and form a conic structure in which the pressure has the highest value. In the simplified form, a QW is a spherical segment whose height (length of the QW) increases with time. The centres of the sparks must not fall in the caverns formed by the preceding sparks since the density of the gas is low in them and the optical breakdown is hampered. A high pressure is created in the QW and in the SW by the last spark at the current instant of time. The pressure in the trailing edge of the QW front pulsates and attains its maximum value at the instant when the next SW catches up with the QW. Since the velocity V_0 of the optical discharge is less than the velocity of sound C_0, while the velocity of the leading front of the QW is equal to C_0, the

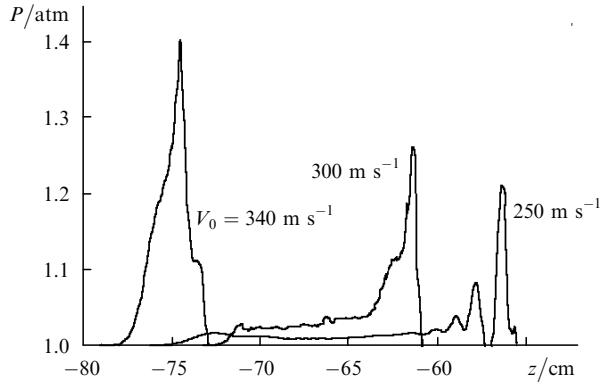

Figure 2. Pressure distribution in the compression phase of a QW on the z axis during the motion of a POD from right to left with different velocities at instants before the ignition of the next spark, when the pressure in the QW over a period between the sparks is minimum, for $R_0 = 1$ cm, $\varepsilon = 25$, and $T_p = 0.15$ ms; $t = 2.1$ ms for $V_0 = 250$ and 340 m s^{-1}, and 1.9 ms for $V_0 = 300$ m s^{-1}.

POD lags behind the leading front after some time and the length of the QW at the instant of its formation (several hundred sparks) increases: $L \sim (C_0 - V_0)t = z(1 - M_0)$, where $M_0 = V_0/C_0$ is the Mach number. It can be assumed that a certainly weakly varying QW structure depending on the velocity and power of POD is established after a fraction of a second.

Figs 2 and 3 show the effect of the velocity and power (different values of V_0 and ε) of a POD on the shape of the QW. The POD power in Fig. 3 is an order of magnitude higher and close to the limiting value. The distribution of pressure along the z axis ($R = 0$) for the instants of time preceding the onset of the next spark is shown. Here, the pressure in the QW is close to its minimum value over a period. The motion of a POD from the point $z = 0$ (to the left) at a velocity $V_0 = 300$ m s^{-1} was simulated. The 'last' spark is located at point $z = -57$ cm ($t = 1.9$ ms), and the centre of the next spark will be located at the point $z = -60$ cm for $t = 2$ ms. The large curvature of the trailing edge of the QW at the segment $z = -63 \div -77$ cm (Fig. 3) is

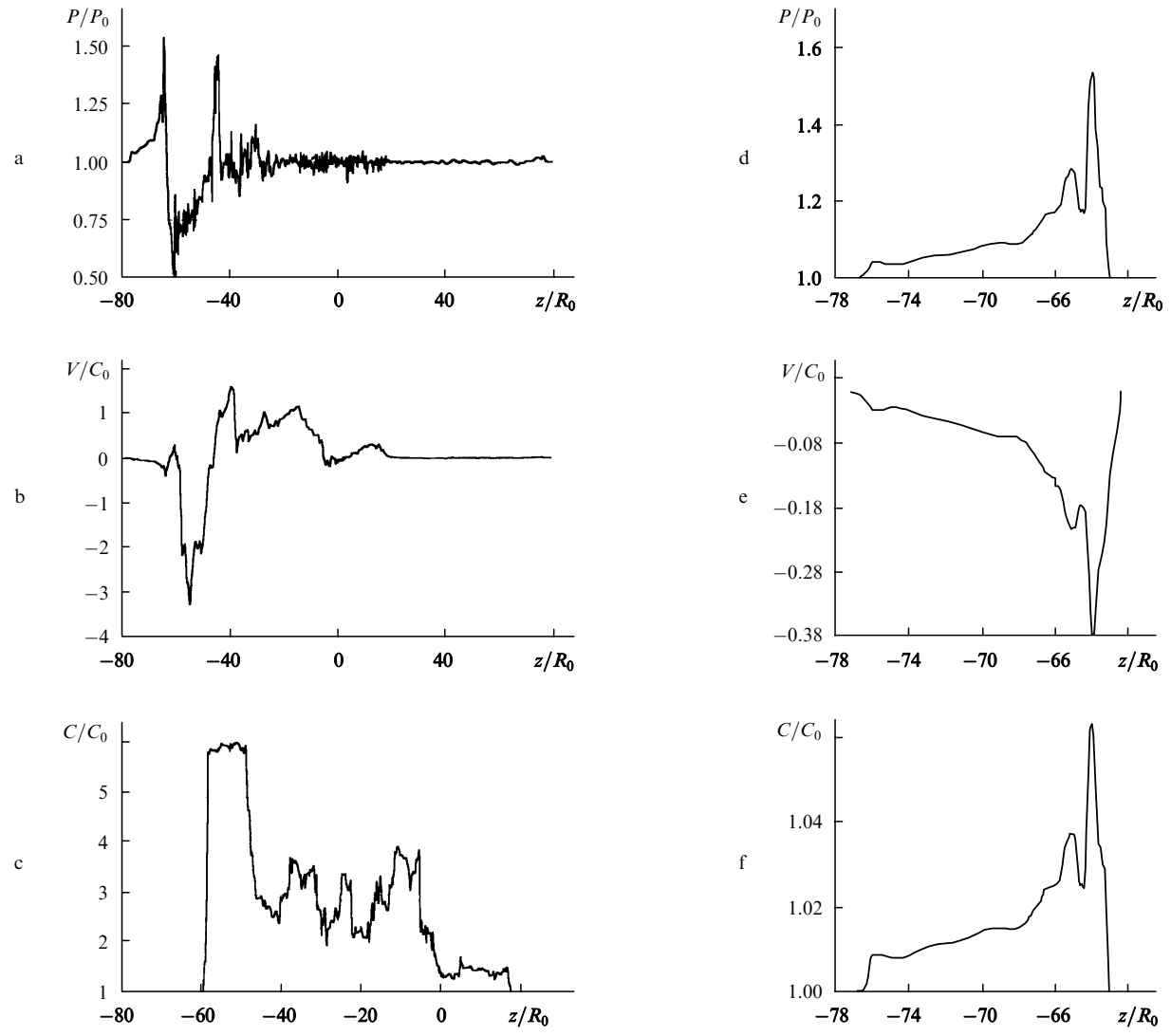

Figure 3. Distribution of pressure P/P_0, velocity of sound C/C_0, and velocity of gas V/C_0 in the plasma trace generated by a POD (a–c) and in a QW (d–f) for $t = 2$ ms, $R_0 = 1$ cm, $V_0 = 300$ m s^{-1}, $f = 10$ kHz, $\varepsilon = 200$ in the first spark and $\sim 90 - 130$ in the next sparks. The decrease in the energy parameter is associated with the fact that absorption takes place at a low density of the gas behind the trailing edge of the QW.

formed by the SW. This is followed (on the right) by a low-pressure region and its jump, which are caused by the last spark. For a high power and small distances between sparks, the POD creates a continuous low-density high-temperature channel. For a SW, the preferred direction is a channel in which the velocity of sound is several times higher than in the surrounding space. The SW in the channel has a compression phase and a low-pressure phase, in which the mass velocities of the gas are directed opposite to each other. The pressure in a channel decreases during the propagation of a SW in it, the radial expansion also playing its part in this. The wave attenuation time is $\sim 0.2-0.3$ ms. The SWs cause the flow of gas in the channel with a velocity $V/C_0 < 1$, which is much lower than the velocity of a jet during the supersonic motion of the POD [12]. The pressure pulsations for $z < 20$ cm shown in Fig. 3a correspond to pulsations in a channel whose length was increased to ~ 20 cm in the positive direction of the z axis. These pulsations are due to the stagnation of the jet at the end of the channel.

One can see from Figs 2 and 3 that the pressure in a SW varies weakly along the z axis in the interval $V_0 \sim 250-300$ m s^{-1}, and an intense peak is formed at the trailing edge as a result of the arrival of a SW. Fig. 4 shows the radial distribution of pressure in a QW in different cross sections along the z axis. A comparison of the data presented in Figs 2 and 3 shows that an increase in the POD power leads to an increase in pressure in a QW whose length depends weakly on power at the initial stage of formation of the QW. Since the velocity of sound in a QW exceeds the velocity of sound in the unperturbed gas ($C > C_0$), the SWs that catch up with the QW propagate in it as small perturbations with a velocity exceeding the velocity of its leading edge. This mechanism of energy transport forms an extended QW region in which the pressure is practically constant. For $t > 1$ ms, the QW pressure pulse acquires a characteristic shape that depends on the difference $C_0 - V_0$ between the velocities. This shape is preserved for at least ~ 4 ms (calculations for longer periods were not carried out). Fig. 5 shows the variation of pressure and velocity of sound at the trailing edge of the QW over a period between sparks. Their rapid growth is associated with the arrival of a SW at the trailing edge of the QW. After this, the SW expands in the QW volume, and hence the pressure and the velocity of sound decrease. It can be seen from Fig. 3 that the gas velocity in the QW may exceed 100 m s^{-1} ($V_0/C_0 \sim 0.38$, $C_0 = 340$ m s^{-1}), while the pressure jump is $\sim 0.1-1.5$ atm.

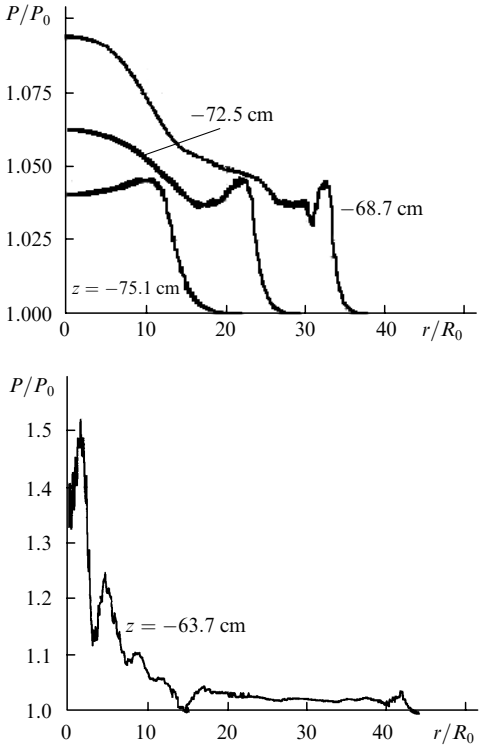

Figure 4. Gas pressure distribution in a QW along the radius in different cross sections along z for the same values of parameters as in Fig. 3.

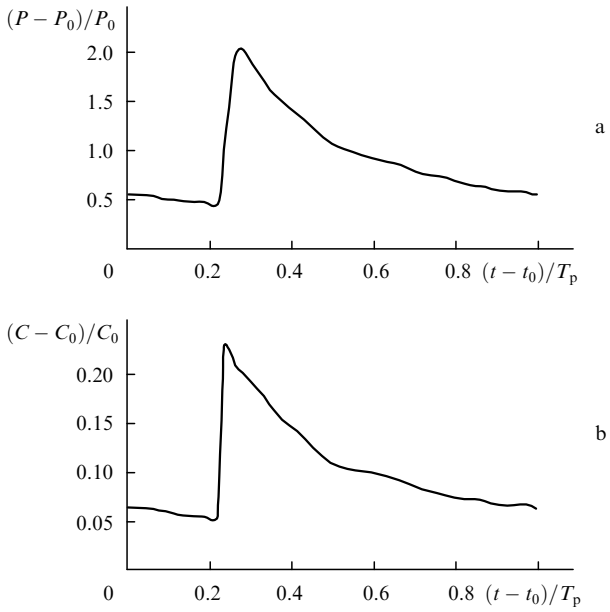

Figure 5. Variation of pressure (a) and the velocity of sound (b) in the region of pressure jump at the trailing edge of the QW for the same values of parameters as in Fig. 3. The time $t_0 = 1.9$ ms corresponds to the instant of ignition of a spark, $T_p = 1/f = 0.1$ ms.

The dependence of the length of a QW and the pressure jumps at its leading and trailing edges on the position of the leading front of the QW are shown in Fig. 6. For a POD moving with a subsonic velocity, the length of the QW increases while the pressure at its leading edge decreases. The pressure at the trailing edge of the QW pulsates, but remains practically unchanged at the same instants of time in a period. If the velocity of the POD is close to the velocity of sound and a high-intensity narrow QW is formed. The energy is extracted in the radial direction. The length of the QW depends linearly on the distance traversed by it, and hence on the energy spent on its formation, in the entire investigated range of POD parameters. This is one of the most significant distinctions between a QW and a SW created, for example, by a single laser spark when the length of the SW depends weakly on the spark energy.

Conditions of formation of a quasistationary wave. Let us determine the parameters for which the laser radiation creates a POD and the SWs generated by it form a QW. We shall determine the required region in a dimensionless form and consider the laser spark as an explosion. After

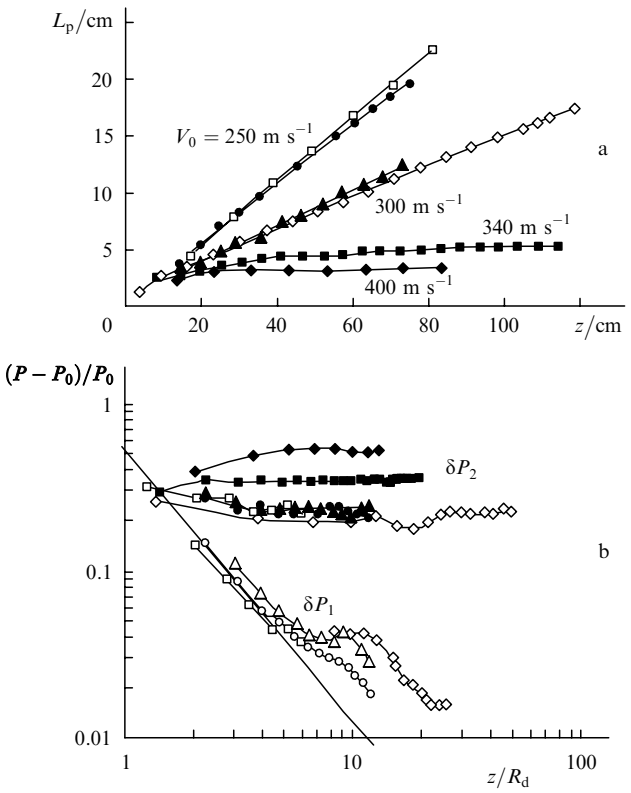

Figure 6. Length of a QW (a) and pressure jump $(P - P_0)/P_0$ in the QW (b) as a function of the position of its leading front for various velocities of the POD ($r = 0$, δP_1 and δP_2 are the pressure jumps at the leading front and the trailing edge of the QW, and R_d is the dynamic radius); $V_0 = 250$ m s^{-1}, $\varepsilon = 25$, $T_p = 0.15$ ms, and $R_0 = 1$ cm (●, ○); $V_0 = 250$ m s^{-1}, $\varepsilon = 250$, $T_p = 0.3$ ms, and $R_0 = 1$ cm (□); $V_0 = 300$ m s^{-1}, $\varepsilon = 25$, $T_p = 0.15$ ms, and $R_0 = 1$ cm (▲, △); $V_0 = 300$ m s^{-1}, $\varepsilon = 50$, $T_p = 0.05$ ms, and $R_0 = 0.3$ cm (◇); $V_0 = 340$ m s^{-1}, $\varepsilon = 25$, $T_p = 0.15$ ms, and $R_0 = 1$ cm (■), and $V_0 = 400$ m s^{-1}, $\varepsilon = 25$, $T_p = 0.25$ ms, and $R_0 = 1$ cm (◆). The solid curve shows the pressure jump in a spherical SW generated by a spark with its centre at the point $z = r = 0$ [the dependence was obtained from formula (5)].

this, we go over to the parameters of the medium and the radiation. The problem involves the following set of independent parameters: pressure P_0 and the velocity of sound C_0 for the unperturbed gas, energy Q_f and duration t_r of the laser pulse, the initial spark radius R_0, the velocity V_0, and the spark repetition period $T_p = 1/f$ for the POD. The value of t_r and the radial energy distribution in a spark do not significantly affect the processes for $t \gg t_r$ if t_r is much smaller than the time T_p, R_0/C_0 and R_0/V_0 (in CO_2 lasers, $t_r \sim 0.5 - 1$ μs). For the dimensionless energy parameter ε, we take the ratio of the energy Q_f and the energy V_f of the unperturbed gas in the spark volume. Taking into account the equation of state for the atmospheric air, the expression for ε has the form

$$\varepsilon = \frac{Q_f}{V_f E_0 \rho_0} = \frac{(\gamma_0 - 1)Q_f}{(4/3)\pi R_0^3 P_0}. \quad (1)$$

Here, E_0 (in J kg^{-1}) is the specific energy of the gas, ρ_0 (in kg cm^{-3}) is its density at $t = 0$, Q_f is measured in joules, R_0 in metres, P_0 in pascals, and $\gamma_0 = 1.4$. The motion of the POD determines the Mach number $M_0 = V_0/C_0$ and the distance between spark centres normalised to the dynamic radius of the explosion (spark), i.e., $Z_n = Z_f/R_d$, where

$$R_d = \left(\frac{Q_f}{P_0}\right)^{1/3} = R_0\left(\frac{4\pi}{3(\gamma_0 - 1)}\,\varepsilon\right)^{1/3} = 2.19 R_0 \varepsilon^{1/3}. \quad (2)$$

The domain of existence of the QW was determined by using characteristic parameters depending on ε, viz., the radius R_c of the cavern formed by the spark as a result of thermal expansion, the length R_s of the shock wave and its period R_p which is equal to the sum of the lengths of the compression and low-pressure phases in the SW. The expressions for R_c, R_s and R_p were obtained from calculations for the spherical case. Three stages can be singled out in an expanding spark. The rapid stage of cavern formation terminates at $t_c/t_0 \simeq 0.43\varepsilon^{0.3}$ ($t_0 = R_0/C_0$), when the pressure at the contact discontinuity becomes equal to P_0. The cavern radius normalised to R_d is given by the expression

$$\frac{R_c}{R_d} = \frac{0.448}{\varepsilon^{0.093}}. \quad (3)$$

For $t_{2c}/t_0 = 0.82\varepsilon^{0.322}$, the pressure is equalised in the entire cavern. In this case, the cavern radius $R_{2c}/R_d = 0.486 \times \varepsilon^{-0.0963}$ and exceeds R_c/R_d by $\sim 10\,\%$, and hence we shall use formula (3) in the subsequent analysis. The velocity of sound in the cavern for t_{2c}/t_0 is equal to $C/C_0 = \varepsilon^{0.34}$. On account of turbulent thermal diffusivity, the gas cools down with a characteristic time ~ 2 ms [6]. The length of the shock wave (compression phase) is

$$\frac{R_s}{R_d} = 0.25\left(\frac{R}{R_d}\right)^{0.33}. \quad (4)$$

The SW period is $R_p/R_d = 1.3(R/R_d)^{0.1}$. For $0.1 < R/R_d < 20$, the pressure jump at the SW front is given by

$$\frac{P - P_0}{P_0} = 0.53\left(\frac{R}{R_d}\right)^{-1.639}. \quad (5)$$

While determining the conditions of existence of the POD, it was assumed that the intensity of laser radiation is higher than the optical breakdown threshold of the gas. It follows from the experiments [13] that radiation is absorbed in the POD if each of the subsequent spark does not fall into the cavern created by the preceding spark, where the gas has a low density. The minimum separation Z_f between the centres of sparks must be larger than the sum of the radii of the spark and the cavern:

$$Z_{sc} > \frac{R_c + R_0}{R_d} = \frac{0.448}{\varepsilon^{0.093}} + \frac{0.457}{\varepsilon^{0.333}}. \quad (6)$$

The right-hand side of this inequality depends weakly on ε (0.448, 0.39, and 0.34 for $\varepsilon = 25$, 100, and 250, respectively). In the following analysis, we shall assume that $Z_{sc} > 0.4$. Shock waves having an initial velocity much higher than C_0 catch up with a QW if the separation between each spark and the trailing edge of the QW is below a certain critical value. This condition is satisfied by displacing the leading edge over a period not exceeding the duration of the SW compression phase. In this case, inequality (6) and the condition for generating a QW assume the following form:

$$Z_{sc} > 0.4, \quad (7)$$

$$M_0 = \frac{V_0}{C_0} < 1, \tag{8}$$

$$(C_0 - V_0)T_p < R_s. \tag{9}$$

Considering the fact that $V_0 T_p = Z_f$, expression (9) assumes the form

$$Z_n < \frac{R_s}{R_d}\frac{M_0}{1 - M_0}. \tag{10}$$

Relation (4) for the SW length can be presented in the form of a power function:

$$\frac{R_s}{R_d} \approx A\left(\frac{R}{R_d}\right)^{\sigma}, \tag{11}$$

where A and σ depend on the properties of the medium in which the QW is formed; R is the distance between the centre of the 'last' spark and the trailing edge of the quasi-stationary wave, at which the SW catches up with the QW. For the sake of definiteness, we assume the following approximate expression: $R \approx bC_0T_p = bZ_f/M_0$, where $b \approx 1-2$ is the fitting factor that will be refined below. In this case, inequality (10) assumes the form

$$Z_n < A^{1/(1-\sigma)} b^{\sigma/(1-\sigma)} \frac{M_0}{(1 - M_0)^{1/(1-\sigma)}}. \tag{12}$$

For air, where $A = 0.25$, $\sigma = 1/3$, and coefficient $b \approx 2$, this expression assumes the form

$$Z_n < 0.177 \frac{M_0}{(1 - M_0)^{1.5}}. \tag{13}$$

This condition was verified in a series of calculations (~ 70 versions) in which all parameters of the POD were varied. Some of the calculated points are shown in Fig. 7. For example, the parameter Z_n was varied by changing the separation Z_f between the spark for fixed values of the relative spark energy ε and its initial radius R_0, as well as for several values of M_0. The boundary points at which the QW formation was observed in calculations are shown in Fig. 7. Periodic SWs generate a low frequency QW in the region bounded by the straight line (*1*) and curve (*2*). The POD is unstable below line (*1*), while the shock waves generated by the POD do not create a quasi-stationary wave above curve (*2*). The light circles show the results of calculations, in which parameters ε (25–250), R_0 (0.3–2 cm), Z_f, and M_0 were varied. In this case also, a QW was formed. The only exceptions are the points $M_0 = 0.588$ (dark and light circles) and $M_0 = 1$ (light circles) at which the conditions for the QW formation are not satisfied. An analysis of the computational data shows that the coefficient of the fraction on the right-hand side of inequality (13) must be increased. The final expressions confining the POD generation region (7) and the regions (8) in which QW is formed in air and (13) (taking corrections into account) assume the form

$$0.4 < Z_n < 0.2 \frac{M_0}{(1 - M_0)^{1.5}}, \tag{14}$$

$$0.56 < M_0 < 1. \tag{15}$$

The left-hand side of the last inequality corresponds to the value of M_0 for which the right-hand side of (14) is equal to 0.4. The right-hand side of (15) limits the velocity of the POD: a low-frequency QW is not formed for $M_0 > 1$. Fig. 7 also shows the experimental data from [41] for underwater explosions of two explosive charges, each of them weighing 0.1 kg. The distance between the charges was $Z_f \sim 25-75$ cm, and the detonation delay time of one charge relative to the other was $T_p = 0.205 - 0.224$ ms. Moving along the axis passing through the charge centres (in the direction of the charge detonating later), the SW generated by the second charge catches up with the first SW, thereby enhancing the pressure significantly in the region of their interaction. The experimental points corresponding to [41] were normalised into dimensionless quantities before being plotted in Fig. 7: $M_0 = Z_f/(T_pC_0) = 0.746 - 0.813$ ($C_0 = 1500$ m s^{-1} is the velocity of sound in water), $Z_n = Z_f/R_d \approx 0.15 - 0.47$, and $R_d \approx 1.7$ m. We did not consider the possibility of increasing the length of the resultant wave in Ref. [41].

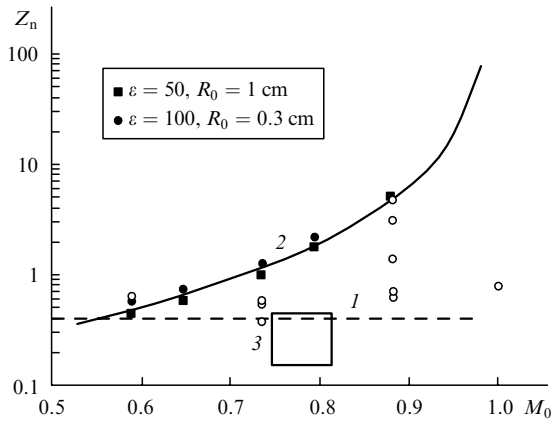

Figure 7. Range of dimensionless parameters in which a POD moving at a velocity $V_0 = M_0C_0$ operates stably, generating a QW in front of it. The range of QWs lies between line (*1*) and curve (*2*). Region (*3*) corresponds to the experimental parameters [41] for which the successive detonation of two charges in water was accompanied by the formation of a unified wave. The symbols on the plane of the figure correspond to our calculations.

A moving POD leaves a trace of low-density ionised gas. If the distance between the spark centres is larger than the diameter of the cavern, i.e., $Z_n \equiv Z_f/R_d > 2R_{2c}/R_d = 0.97/\varepsilon^{0.0963}$, the trace is formed by caverns isolated from one another. The value of $2R_{2c}/R_d = 0.727 - 0.582$ for $\varepsilon = 20 - 200$. The POD leaves a trace in the form of a continuous channel if the distance between the centres of sparks is smaller than the sum of the radii of the cavern and the laser spark: $Z_p \leqslant (R_c + R_0)/R_d \approx 0.4$. Here, the gas in the channel moves in a direction opposite to that of the POD with a velocity $V \sim 200 - 500$ m s^{-1}. It should be noted that for a POD moving at a supersonic speed, the velocity of the ionised gas in the channel is limited by the velocity of sound in it and may attain values of the order of 2–3 km s^{-1} [12]. In the region of transition from a discontinuous trace to a continuous one, there exists a narrow region of POD parameters, in which the gas moves in the same direction as the POD.

Let us present the range of QWs in terms of the laser radiation parameters. We consider two cases. Suppose that the average power W_f of laser radiation, velocity V_0 of the POD, pressure P_0, and velocity C_0 of sound in the gas are known. It is required to find the energy Q_f and the repetition rate f of laser pulses, for which the POD operates and creates a QW in front of it. Using formula (2) and the obvious relations for $Z_f = V_0/f$ and $W_f = Q_f f$, we obtain from (14) the following relations for Q_f and f:

$$8 \times 10^{-4} \frac{(W_f/P_0)^{1.5}}{(C_0 M_0)^{1.5}} < \frac{Q_f}{P_0} < \frac{2.83 \times 10^{-4} (W_f/P_0)^{1.5}}{C_0^{1.5}(1-M_0)^{2.25}}, \quad (16)$$

$$\frac{3534 C_0^{1.5}(1-M_0)^{2.25}}{(W_f/P_0)^{0.5}} < f \leqslant 1250 \frac{(C_0 M_0)^{1.5}}{(W_f/P_0)^{0.5}}. \quad (17)$$

Here, as well as in the following relations (18) and (19), P_0 is measured in atmospheres, C_0 in m s^{-1}, W_f in watts, Q_f in joules, and f in hertzs. Similarly, inequality (14) leads to the following expressions for the range of the average power and the repetition rate f of laser pulses, for which a POD exists and creates a QW for given values of Q_f, V_0, P_0, and C_0:

$$232 C_0 (1-M_0)^{1.5} \left(\frac{Q_f}{P_0}\right)^{2/3} < \frac{W_f}{P_0} < 116 M_0 C_0 \left(\frac{Q_f}{P_0}\right)^{2/3}, \quad (18)$$

$$\frac{232 C_0 (1-M_0)^{1.5}}{(Q_f/P_0)^{1/3}} < f < 116 \frac{M_0 C_0}{(Q_f/P_0)^{1/3}}. \quad (19)$$

Expressions (16)–(19) are illustrated in Figs 8 and 9. The parts of the inequalities containing the factor $1 - M_0$ correspond to the condition of the QW formation [curves (*1*) and (*1′*)], while the remaining parts, containing the factor M_0, correspond to the condition for the existence of a POD [lines (*2*) and (*2′*)]. A QW will be formed for any values of the parameters lying between curves (*1*) and (*2*) [(*1′*) and (*2′*)] and for $M_0 = 0.57 - 1$. No low-frequency wave is formed for $M_0 > 1$. It is assumed that the laser radiation intensity is higher than the breakdown threshold of the gas. Fig. 8 shows the values of Q_f and f for an average POD power $W_f = 2$ and 10 kW. It can be assumed that the former value ($W_f = 2$ kW) corresponds to the formations of a QW in inert gases, in which the optical breakdown threshold is lower than in air. The POD described in Ref. [13] operated in argon for $Q_f \approx 0.01$ J (CO_2 laser). The breakdown threshold in air is $\sim 0.1 - 2$ J [42] and depends on the radiation wavelength, pulse duration, focal length, and the concentration of aerosols. A laser radiation with an average power of ~ 10 kW and higher is required for generating a QW in air. Fig. 9 shows the average POD power and the pulsation frequency for fixed values $Q_f = 1$ and 10 J of the energy of a spark.

Shock waves with a large value of L are interesting (Earth sounding, hydroacoustics) owing to their weak damping [33–37, 43]. The length of the SW generated by a solitary spark or an explosion depends weakly on energy [44, 45]. The energy expenditure increases sharply with L (as

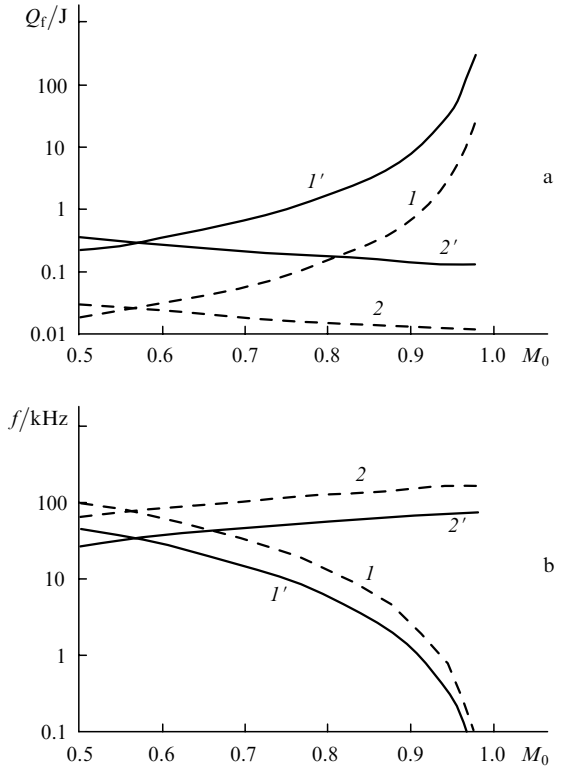

Figure 8. Ranges of a stable POD generating a QW for $C_0 = 340$ m s^{-1}, $P_0 = 1$ atm, $M_0 = 0.57 - 1$, and $W_f = 2$ kW [curves (*1*) and (*2*)] and 10 kW [curves (*1′*) and (*2′*)]. Curves (*1*) and (*1′*) correspond to the condition for the QW formation, while (*2*) and (*2′*) correspond to the stable POD operation condition.

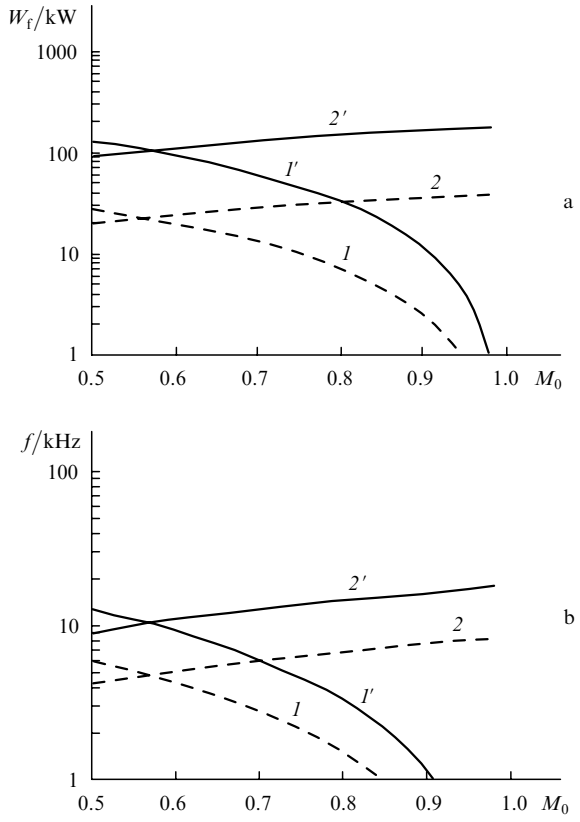

Figure 9. Ranges of a stable POD generating a QW for $C_0 = 340$ m s^{-1}, $P_0 = 1$ atm, $M_0 = 0.57 - 1$, and $Q_f = 1$ J [curves (*1*) and (*2*)] and 10 J [curves (*1′*) and (*2′*)]. The POD is unstable above the lines (*2*) and (*2′*), while the SWs generated by the POD do not create a QW below curves (*1*) and (*1′*).

$L^{9/2}$ for a spherical SW). Moreover, the shape of the SW is close to spherical in free space as a rule. Like any other nonspherical wave, a directed wave can be obtained only in the near-field region [46]. The SW is free from such drawbacks as it moves along the beam and its length L depends linearly on the energy spent on generating a QW.

Thus, a pulsed optical discharge moving in a gas at a subsonic velocity generates in front of it a low-frequency QW propagating along the laser beam at the velocity of sound in the same direction as the POD. A QW is a flow of gas with a velocity as high as ~ 100 m s^{-1} and a pressure of several atmospheres. This effect is based on a high energy density in laser sparks and a high pulsation frequency of the POD. The mechanism of the QW formation can be described as follows: a low-frequency wave is generated for a point-sized POD in the surrounding gas as a result of the interaction of periodic SWs generated by the POD. In contrast to the SW pressure, the pressure in a QW is maximum at the trailing edge, while the length of the QW increases linearly with the energy spent on its generation. A QW can be defined as a special type of compression waves, which, unlike ordinary compression waves, are not transformed into SWs as long as a POD exists. The range of radiation parameters for which a stable POD operates and creates a QW is obtained in dimensionless form.

Acknowledgements. This work was supported by the Russian Foundation for Basic Research (Grant No. 03-02-17716). The author thanks A.G. Ponomarenko for supporting this research and for discussion of the results. Thanks are also due to A.I. Gulidov who developed the software for computations.

References

1. Myrabo L.N., Raizer Yu.P. *AIAA Paper* (94-2451) (1994).
2. Chtrnyi G.G. *Proc. of the II Weakly Ionized Gases Workshop* (Norfolk, USA, 1998; Norfolk: Amer. Inst. Aeronaut. and Astronaut., 1998) pp 1 – 31.
3. Georgievskii P.Yu., Levin V.A. *Pis'ma Zh. Tekh. Fiz.*, **14** (8), 684 (1988).
4. Tret'yakov P.K., Grachev G.N., Ivanchenko A.I., Krainev V.L., Ponomarenko A.G., Tishchenko V.N. *Dokl. Akad. Nauk*, **336** (4), 466 (1994).
5. Tret'yakov P.K., Garanin A.F., Grachev G.N., Krainev V.L., Ponomarenko A.G., Tishchenko V.N. *Dokl. Akad. Nauk*, **351** (3), 339 (1996).
6. Tischenko V.N., Antonov V.M., Melekhov A.V., Nikitin S.A., Posukh V.G., Shaikhislamov I.F. *J.Phys. D: Appl. Phys.*, **31**, 1998 (1998).
7. Tishchenko V.N. *Optika Atmos. Okeana*, **11** (2 – 3), 228 (1998).
8. Generalov N.A., Zimakov V.P., Kozlov G.I., Masyukov V.A., Raizer Yu.P. *Zh. Eksp. Teor. Fiz.*, **61**, 1434 (1971).
9. Raizer Yu.P. *Lazernaya iskra i rasprostranenie zaryadov* (Laser Spark and Charge Propagation) (Moscow: Nauka, 1974).
10. Gerasimov M.V., Kozlov G.I., Kuznetsov V.A. *Kvantovaya Electron.*, **10**, 709 (1983) [*Sov. J. Quantum Electron.*, **13**, 438 (1983)].
11. Grachev G.N., Ponomarenko A.G., Smirnov A.L., Tischenko V.N., Tret'jacov P.K. *Laser Phys.*, **6**, 376 (1996).
12. Tishchenko V.N., Gulidov A.I. *Pis'ma Zh. Tekh. Fiz.*, **26** (19), 77 (2000).
13. Tishchenko V.N., Grachev G.N., Zapryagaev V.I., Smirnov A.V., Sobolev A.V. *Kvantovaya Electron.*, **32**, 329 (2002) [*Quantum Electron.*, **32**, 329 (2002)].
14. Bufetov I.A., Prokhorov A.M., Fedorov V.B., Fomin V.K. *Dokl. Akad. Nauk SSSR*, **261**, 586 (1981).
15. Kondrashov V.N., Rodionov N.B., Sitnikov S.F., Sokolov V.I. *Issledovanie gazodinamicheskikh effektov na pozdnikh stadiyakh lazernoi iskry* (Investigation of Gasdynamic Effects at Later Stages of Laser Spark) Preprint No. 4154/7, (Moscow, Atomic Energy Institute, 1985).
16. Bunkin F.V., Komissarov V.M. *Akustich. Zh.*, **19** (3), 307 (1973).
17. Ostrovskaya G.V., Zaidel' A.N. *Usp. Fiz. Nauk*, **111**, 579 (1973).
18. Bufetov I.A., Prokhorov A.M., Fedorov V.B., Fomin V.K. *Trudy IOFAN*, **10**, 3 (1988).
19. Manzon B.M. *Zh. Tekh. Fiz.*, **54**, 2283 (1984).
20. Anisimov V.N., Vorob'ev V.A., Grishina V.G., Derkach O.N., Kanevskii M.F., Sebrant A.Yu., Stepanova M.A., Chernov S.Yu. *Kvantovaya Electron.*, **22**, 862 (1995) [*Quantum Electron.*, **25**, 831 (1995)].
21. Bozhkov A.I., Bunkin F.V., Savranskii V.V. *Pis'ma Zh. Tekh. Fiz.*, **1** (9), 435 (1975).
22. Bozhkov A.I., Bunkin F.V. *Kvantovaya Electron.*, **2**, 1763 (1975) [*Sov. J. Quantum Electron.*, **5**, 956 (1975)].
23. Bunkin F.V., Mikhalevich V.G., Shipulo G.P. *Kvantovaya Electron.*, **3**, 441 (1976) [*Sov. J. Quantum Electron.*, **6**, 238 (1976)].
24. Bunkin F.V., Tribel'skii M.I. *Usp. Fiz. Nauk*, **130** (2), 193 (1980).
25. Kozev E.F., Naugol'nykh K.A. *Akustich. Zh.*, **22**, 366 (1976).
26. Kasoev S.G., Lyamshev L.M. *Akustich. Zh.*, **23**, 608 (1977).
27. Lyamshev L.M., Mikhalevich V.G., Shipulo V.G. *Akustich. Zh.*, **25**, 146 (1979).
28. Lyamshev L.M., Mikhalevich V.G., Shipulo V.G. *Akustich. Zh.*, **26**, 230 (1980).
29. Lyamshev L.M. *Usp. Fiz. Nauk*, **135**, 637 (1981).
30. Golubev S.A., Kovalev A.S., Mikhailova N.V., Myshetskaya E.E., Persiantsev I.G., Pis'mennyi V.D., Rakhimov A.T., Favorskii A.P. *Dokl. Akad. Nauk SSSR*, **225**, 1300 (1975).
31. Baranov V.Yu., Lyubimov B.Ya., Niz'ev V.G., Pigul'skii S.V. *Kvantovaya Electron.*, **6**, 177 (1979) [*Sov. J. Quantum Electron.*, **9**, 97 (1979)].
32. Tishchenko V.N., Grachev G.N., Gulidov A.I., Zapryagaev V.I., Posukh V.G. *Kvantovaya Electron.*, **31**, 283 (2001) [*Quantum Electron.*, **31**, 283 (2001)].
33. Egerev S.V., Lyamshev L.M., Naugol'nykh K.A. *Akustich. Zh.*, **36** (5), 807 (1990).
34. Polyakova A.L., Sil'vestrova O.Yu. *Akustich. Zh.*, **36** (5), 814 (1990).
35. Donskii D.M., Zaitsev V.Yu., Naugol'nykh K.A., Sutin A.M. *Akustich. Zh.*, **39** (2), 266 (1993).
36. Esipov I.B., Kalachev A.I., Sokolov A.D., Sutin A.M., Sharonov G.A. *Akustich. Zh.*, **39** (3), 377 (1993).
37. Naugol'nykh K.A., Ostrovskii L.A., Sutin A.M., in *Nelineinie volny. Rasprostranenie i vzaimodeistvie* (Nonlinear Waves. Propagation and Interaction) (Moscow: Nauka, 1981) p. 166.
38. Fomin V.M., Gulidov A.I., Sapozhnikov G.A. *Vysokoskorostnoe vzaimodeistvie tel* (High-speed Interaction between Bodies) (Novosibirsk: Izd. Sib. Otd. RAN, 1999).
39. Kuznetsov N.M. *Termodinamicheskie funktsii i udarnie adiabaty vozdukha pri vysokikh temperaturakh* (Thermodynamic Functions and Shock Adiabats of Air at High Temperatures) (Moscow: Mashinostroenie, 1965).
40. Markelova L.P., Nemchinov N.V., Shubadeeva L.P. *Zh. Priklad. Mekh. Tekh. Fiz.*, (2), 54 (1973).
41. Stebnovskii S.V. *Zh. Priklad. Mekh. Tekh. Fiz.*, (4), 87 (1978).
42. Zuev V.E. *Opticheskii razryad v aerozolyakh* (Optical Discharge in Aerosoles) (Novosibirsk, Nauka, 1990).
43. Kedrinskii V.K. *Underwater Explosives Sound Sources. Encyclopaedia of Acoustics*. Ed. by M.J. Crocker. (New York, Toronto: John Wiley and Sons, 1997) Vol. 1, p. 539.
44. Korobeinikov V.P. *Zadachi teorii tochechnogo vzryva* (Problems in the Theory of Point Explosions) (Moscow: Nauka, 1985).
45. Yakovlev Yu.S. *Gidrodinamika vzryva* (Hydrodynamics of Explosions) (Leningrad: GIZ, 1961).
46. Pinaev A.V., Kuzakov V.T., Kedrinskii V.K. *Zh. Priklad. Mekh. Tekh. Fiz.*, (5), 81 (2000).